Desalination and Water Treatment
www.deswater.com

doi: 10.1080/19443994.2015.1048533

57 (2016) 12264–12273
June

Taylor & Francis
Taylor & Francis Group

Novel organic dye sorbent: synthesis and adsorption properties of multi-walled carbon nanotubes modified with gallic amide units

Sining Zheng[a], Hongyu Guo[a], Fafu Yang[a,b,*], Biqiong Hong[a]

[a]*College of Chemistry and Chemical Engineering, Fujian Normal University, Fuzhou 350007, P.R. China, Tel./Fax: +86 591 83465225; emails: 278730134@qq.com (S. Zheng), guohongyuyang@126.com (H. Guo), yangfafu@fjnu.edu.cn (F. Yang), 316029243@qq.com (B. Hong)*

[b]*Fujian Key Laboratory of Polymer Materials, Fujian Normal University, Fuzhou 350007, P.R. China*

Received 22 October 2014; Accepted 3 May 2015

ABSTRACT

By reacting acyl chloride-MWCNTs with gallic amino derivative containing three long alkyl chains, novel gallic-MWCNTs **4** was prepared in good yield. Its structure was characterized by Fourier translation infrared spectroscopy, Raman spectroscopy, X-ray diffraction, scanning electron microscopy, and thermogravimetric analysis. The gallic derivative content of gallic-MWCNTs was 14.5 wt%. Its adsorption experiments for four cationic and anionic dyes [Orange G sodium salt (OG), Brilliant ponceau 5R (BP), Neutral red (NR), and Methylene blue (MB)] were investigated. The adsorption process attained to adsorption equilibrium in 2.5 h under the condition of 5.0 mg of sorbent in dye solutions (10 mL, 2.0×10^{-3} M) in the thermostatic shaker bath with a shaking of 200 rpm at 25°C. The saturated adsorption capabilities were 0.642 mmol/g (289 mg/g), 0.537 mmol/g (324 mg/g), 0.891 mmol/g (256 mg/g), and 0.823 mmol/g (310 mg/g), respectively. The adsorption processes were exothermic and spontaneous, and obeyed pseudo-second-order model and the Langmuir isotherm equation. The adsorption capacities for anionic dyes (OG and BP) decreased with the increase in the pH values of solution and the adsorption capacities for cationic dyes (NR and MB) showed reverse changes.

Keywords: Carbon nanotube; Gallic; Adsorption; Dye

1. Introduction

Synthetic dyes exist widely in wastewater of various industries including textiles, leather, dyestuffs, papers, etc. They can seriously do harm to biodiversity and the natural activities of aquatic systems [1]. Hence, the removal of dye from wastewater is an important environment issue. Up to now, various types of conventional treatment processes including chemical coagulation, precipitation, adsorption, membrane filtration, photodegradation etc., have been studied in removing the dyes from wastewaters [2–5]. Adsorption has been found to be superior to other techniques for treating wastewater because it is simple, convenient, and low cost with high adsorption efficiency and wide adaptability [6–8].

Since the discovery of carbon nanotubes (CNTs) in 1991, they have exhibited potential application in adsorption removal of various pollutants such as metallic ions and synthetic dyes based on their large specific surface area, nanometer size, and hollow-layered

*Corresponding author.

structures [9–12]. Fagan and his co-workers studied the adsorption of Reactive Blue 4 dye from water solutions by CNTs [13]. Wu investigated the equilibrium, kinetics, and thermodynamics of adsorption of reactive dye onto CNTs [14]. Wang et al. reported the synergistic and competitive adsorption of organic dyes on multi-walled carbon nanotubes (MWCNTs) [15]. Yao etc. described the dyes adsorption properties of CNTs and MWCNTs [16,17]. However, some obvious obstacles of raw CNTs, such as self-aggregating resulting in poor dispersion in solvents and lack of surface functional groups for selectively adsorption with guests, greatly restricted their actual application in the removal of pollutants [18]. Thus, the modifications of CNTs with other molecules were extensively investigated recently to enhance the dispersion and obtain outstanding adsorption properties. For example, the chitosan-modified MWCNTs showed highly effective removal of a carcinogenic dye [19]. The starch-functionalized CNTs were reported as excellent sorbent for dyes [10]. A cyclodextrin-CNT composite was prepared and its adsorption properties for dyes were also investigated lately [20]. These investigations suggested that the adsorption properties of CNTs with functional groups were greatly influenced by the structures and amounts of functional groups on CNTs. Gallic amides with three alkyl chains on the 3,4,5-positions are planar aromatic structures, which has good affinity for organic dyes with planar aromatic structures. It is expected that the introduction of gallic amide with three alkyl chains onto CNTs would improve the dyes adsorption properties apparently. Based on these considerations, in this paper, we designed and synthesized the first example of gallic amide-modified multi-walled CNTs (gallic-MWCNTs). Its structure was characterized by Raman spectroscopy, FT-IR, X-ray diffraction (XRD), scanning electron microscopy (SEM), and thermogravimetric analysis (TG). The adsorption abilities for dyes were studied. The results indicated that this novel carbon nanomaterial showed excellent dyes adsorption capabilities comparing with raw CNTs as expected.

2. Experimental

2.1. Materials and measurements

Carboxyl MWCNTs (Purity > 95 wt%, COOH content: 1.23 wt%, OD: 20–30 nm, Length 10–30 μm, SSA: > 110 m^2/g) were provided by Chengdu Organic Chemicals Co. Ltd, Chinese Academy of Sciences, China. ^1H NMR spectra were recorded in $CDCl_3$ on a Bruker-ARX 600 instrument at room temperature, using TMS as an internal standard. ESI-MS spectra were obtained from DECAX-30000 LCQ Deca XP mass spectrometer. IR spectra were recorded on Perkin-Elmer 1605 FTIR spectrometer as KBr pellets. UV–vis measurements were performed on a Varian UV–vis instrument. Surface morphology of carboxyl MWCNTs and gallic-MWCNTs were studied using SEM (JEOLJSM-6490LA). XRD experiments were performed on SEIFERT-FPM (XRD7), using Cu Kα 1.5406 Å as the radiation source with 40 kV, 30 mA power. Thermal properties were measured using a ZTY-ZP type thermal analyzer. Samples were heated from room temperature to 800°C at a heating rate of 15°C/min in nitrogen atmosphere. Raman spectra were recorded on a Renishaw InVia Reflex Raman microscope (Renishaw Instruments) using a 532 nm argon ion laser. All dyes were purchased from Acros Organics, China. Their structures and λ_{max} of absorbing

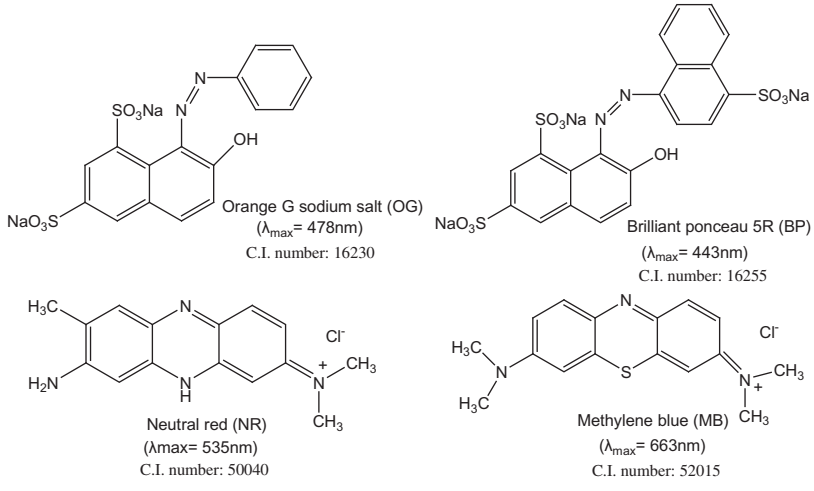

Fig. 1. The structures of cationic and anionic dyes for absorption experiments.

wavelength were shown in Fig. 1. Compound **2** was prepared by literature method [21]. All solvents were purified by standard procedures before use. The other chemicals, except those with special instruction, were analytically pure and used without further purification. All reactions were carried out under nitrogen atmosphere.

2.2. Preparation of compound 3

Compound **2** (0.69 g, 1 mmol) was refluxed with 1 mL of ethylenediamine in 15 mL of methanol for 8 h. TLC detection suggested the disappearance of compound **2**. Then the solvent was evaporated under reduced pressure and the residue was recrystallized in $MeOH/CHCl_3$. Compound **3** was obtained as white soft solid in yield of 86%. Compound **3**: ^1H NMR (400 MHz, $CDCl_3$) δppm: 0.89 (bs, 9H, CH_3), 1.26–1.79 (m, 60H, CH_2), 2.15 (s, 2H, NH_2), 3.12 (bs, 2H, CH_2), 3.44 (bs, 2H, CH_2), 3.95 (bs, 6H, CH_2), 7.04 (s, 2H, ArH), 7.21 (bs, 1H, NH); MS m/z (%): 717.2 (M^+, 100). Anal. calcd for $C_{45}H_{84}N_2O_4$: C 75.36, H 11.81, N 3.91; found C 75.41, H 11.86, N 3.87%.

2.3. Preparation of gallic-MWCNTs 4

A sample of compound **3** (0.3 g, 0.42 mmol) and triethylamine (0.2 mL) was dissolved in 20 mL of dry DMF for next step. Under nitrogen atmosphere, carboxyl MWCNTs (0.3 g, 0.082 mmol of COOH groups), $SOCl_2$ (0.5 mL) was dispersed in 20 mL of dry DMF using ultrasonication for 10 min to obtain a homogeneous dispersion and then 0.5 mL of $SOCl_2$ was added in it. The obtained DMF solution was stirred at 100°C overnight. After reaction, the solvent and excess of $SOCl_2$ were removed under reduced pressure. Then the previous prepared DMF solution of compound **3** with triethylamine was added in dropwise and subsequently stirred at 90°C for 24 h. After reaction, the mixture was cooled to room temperature and 30 mL of distilled water was added. Then the mixture was centrifuged, washed with acetone for three times to remove the small molecules. Finally, the black gallic-MWCNTs **4** (0.33 g) was obtained after dryness in an oven at 100°C for 3 h.

2.4. Adsorption of dyes

Referring to published methods [22], the adsorption properties of gallic-MWCNTs **4** were studied for cationic and anionic dyes shown in Fig. 1. Except the investigation for the effect of times on adsorption, all adsorption experiments were done in the thermostatic shaker bath with a shaking of 200 rpm at 25°C for 24 h. For kinetic studies, dye solutions (10 mL, 2.0×10^{-3} M) were agitated with 5.0 mg of sorbent for predetermined intervals of time, respectively. For equilibrium adsorption studies, 5.0 mg of gallic-MWCNTs **5** was added into a known concentration ($1.0–10 \times 10^{-3}$ M) of 10 mL dye solutions. Because the pH studies of sorption experiment (in Fig. 9) showed no optimized pH between pH 3–10, all these kinetics, equilibrium, and thermodynamic studies of adsorption experiments were done at their original pH values (5.5 for OG, 5.3 for BP, 7.0 for NR, 7.5 for MB), avoiding the changes in structures of dyes at high or low pH values because of the protonation or ionization of dyes. The changes in pH values before and after the adsorption were only 0.1–0.2, indicating the structures of dyes kept stable before and after the adsorption. After filtration, the concentration of each dye solution was determined by vis–UV measurement. The amount of adsorbed dyes was calculated as follows Eq. (1):

$$q = (C_0 - C)V/m \tag{1}$$

where q is the amount of absorbed dyes (mmol/g); C_0 is the known concentration of dyes before adsorption (mmol/L); and C is the concentration of dyes after adsorption (mol/L). Average of two independent experiments was carried out. V is the volume of dyes aqueous solution (L) and m is the dose of sorbent (g).

3. Results and discussion

3.1. Synthesis and characteristic of gallic-MWCNTs 4

The synthetic route of gallic-MWCNTs **4** was shown in Fig. 2. Compound **2** was prepared according to published method [21]. Ammonolysis of compound **2** with ethylenediamine gave gallic amino derivative **3** in yield of 86%. On the other hand, by treating with excess $SOCl_2$, the carboxyl group of carboxyl MWCNTs was transformed to acyl chloride. Then by reacting the acyl chloride-MWCNTs with gallic amino derivative **3**, the target gallic-MWCNTs **4** was prepared by the ammonolysis of acyl chloride. In order to convert carboxyl groups to amido groups as much as possible, the excess of compound **3** (0.42 mmol for NH_2 groups) was reacted with carboxyl MWCNTs (0.082 mmol for COOH groups). After reaction, the excess of compound **3** was removed easily by washing with acetone. Totally, the gallic-MWCNTs **4** was obtained with the simple separating procedure in good yield. The structure and morphology of gallic-MWCNTs **4** was characterized by FTIR, XRD, SEM, TG, and Raman microscope, etc.

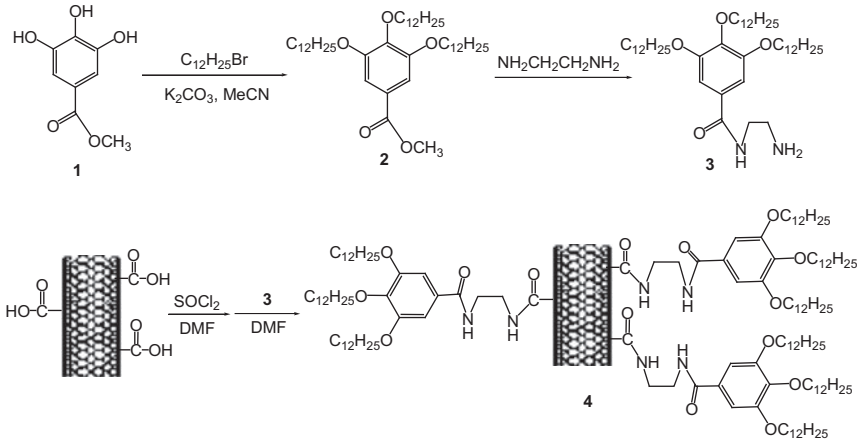

Fig. 2. The preparation of MWCNTs modified with gallic amide containing three long alkyl chains.

The TG for carboxyl MWCNTs and gallic-MWCNTs **4** were investigated and the results were shown in Fig. 3. The carboxyl MWCNTs almost had no loss of mass between room temperature and 700˚C. The thermal decomposition temperature of gallic-MWCNTs **4** was 300˚C approximately, which was similar to that of gallic derivative **3**. Moreover, gallic-MWCNTs **4** exhibited a weight loss of 12 wt% at 200–400˚C. According to the reported method to calculate the content of grafting units by TGA [10,20], it was assumed that the mass loss of gallic derivative **3** at the decomposed temperature was still constant when it was introduced onto carboxyl MWCNTs. Thus, the quantity of gallic derivative **3** was calculated by matching the percent weight loss of gallic-MWCNTs **4** to the percent weight loss of gallic derivative **3** at the decomposition temperature (83 wt%). The calculating formula was as follows: the content = 12/83% = 14.5 wt%. The gallic derivative content of gallic-MWCNTs was estimated to be about 14.5 wt% after calculation. This content was similar to the content of the other analogical functional MWCNT, such as starch-functionalized CNTs [10] and cyclodextrin-composited CNTs [20].

The structure of gallic-MWCNTs **5** was also confirmed by IR spectrum as shown in Fig. 4. Comparing with the IR spectra of carboxyl MWCNTs, the IR spectrum of gallic-MWCNTs **5** showed new peak at 1,649 cm^{-1} for C=O of amide groups instead of the peak at 1,709 cm^{-1} for C=O of carboxyl MWCNTs. The absorption peaks at 2,800–3,000 cm^{-1} for C–H groups were observed clearly in the IR spectrum of gallic-MWCNTs **4**. These data of IR spectra certainly suggested that the gallic units were grafted onto MWCNTs and the carboxyl of MWCNTs were converted to amide groups mostly.

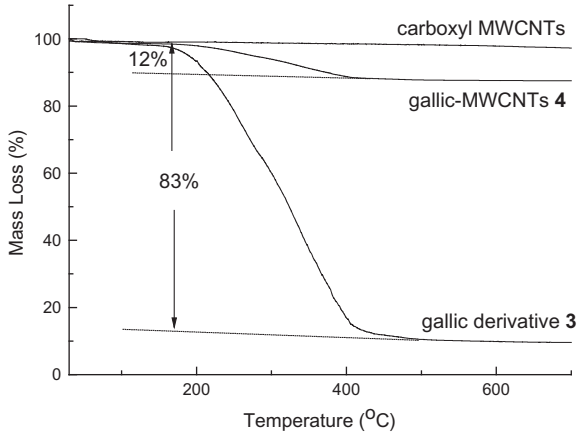

Fig. 3. TG curves of carboxyl MWCNTs, gallic derivative **3**, and gallic-MWCNTs **4**.

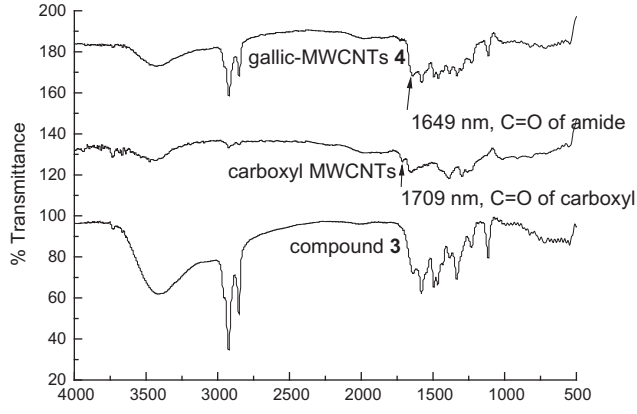

Fig. 4. IR spectra of carboxyl MWCNTs, compound **3**, and gallic-MWCNTs **4**.

The Raman spectra of the carboxyl MWCNTs and gallic-MWCNTs **4** were studied and the results were shown in Fig. 5. The peaks at 1,310 and 1,595 cm^{-1} were assigned for the disordered structure of MWCNTs (D mode) and for the graphite structure of MWCNTs (G mode), respectively. Usually, the G band arises from the E_{2g} phonon of sp^2 atoms, and the D band is a breathing mode of *k*-point phonons of A_{1g} symmetry. The intensity ratio (I_D/I_G) of the D band to the G band was used to confirm the size of sp^2 domains in graphitic materials [23]. In Fig. 5, the I_D/I_G ratios were 1.9824 for carboxyl MWCNTs and 2.6037 for gallic-MWCNTs **4**. Comparing with carboxyl MWCNTs, the slightly increased I_D/I_G ratio for gallic-MWCNTs **4** suggested a decrease in the size of the sp^2 domains. This result implied that the degree of disorder on the surfaces gallic-MWCNTs **4** increased and the gallic units were grafted onto MWCNTs successfully.

The XRD analysis was employed to study the structures of carboxyl MWCNTs and gallic-MWCNTs **4**. The results were shown in Fig. 6. It can be seen that carboxyl MWCNTs and gallic-MWCNTs **4** exhibited similar diffraction peaks at $2\theta = 25$ and 43°, indicating that the attachment of gallic units on MWCNTs did not destroy the framework of the CNT structure [20]. Comparing with carboxyl MWCNTs, the intensity of peaks of gallic-MWCNTs **4** became weaker, which could be attributed to the steric hindrance of gallic units for the stacking of MWCNTs. This result suggested the reduction in the self-aggregation of MWCNTs, which was favorable for increasing the dispersion in solvents and enhancing dye adsorption.

The surface morphologies of carboxyl MWCNTs and gallic-MWCNTs **4** were also investigated by SEM images. They showed similar entangled tube morphology, indicating the graft of gallic units on MWCNTs did not destroy the framework of the CNT structure, which was in accordance with the XRD results.

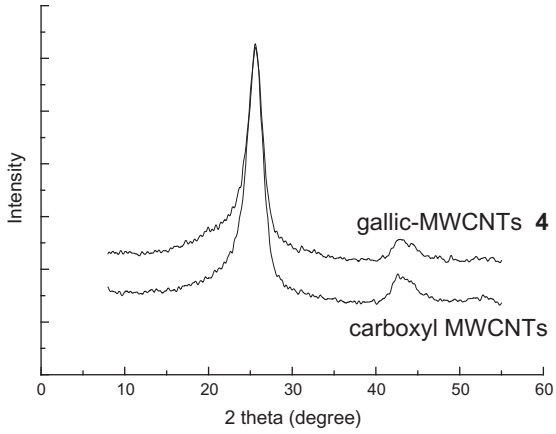

Fig. 6. XRD patterns of carboxyl MWCNTs and gallic-MWCNTs **4**.

3.2. Adsorption kinetics

Four normal cationic and anionic dyes [Orange G sodium salt (OG), Brilliant ponceau 5R (BP), Neutral red (NR), and Methylene blue (MB)] were chosen to investigate the adsorption abilities of novel gallic-MWCNTs **4**. The q_t values vs. the contact time on carboxyl MWCNTs and gallic-MWCNTs **4** were shown in Figs. 7 and 8. One can see that adsorption process happened quickly in the initial stage and attained to adsorption equilibrium in 2 and 2.5 h for carboxyl

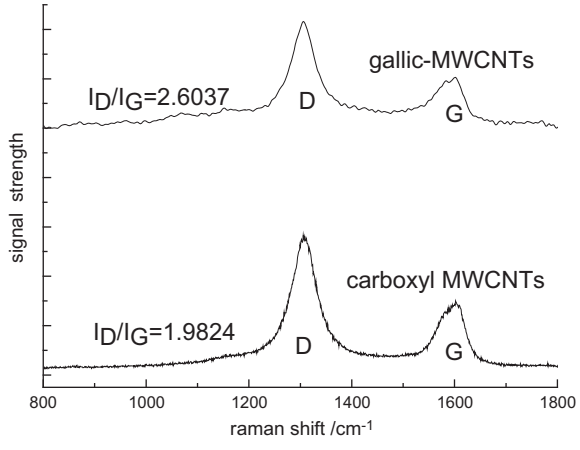

Fig. 5. Raman spectra of carboxyl MWCNTs and gallic-MWCNTs **4**.

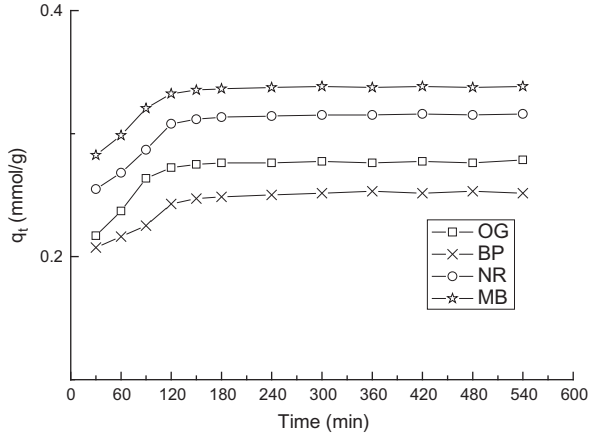

Fig. 7. Effect of adsorption time on dye adsorption by carboxyl MWCNTs.

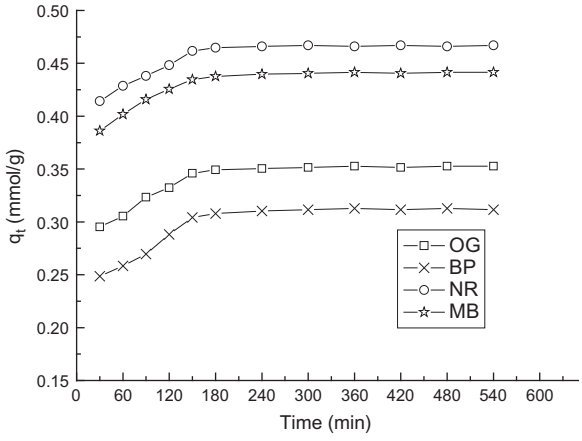

Fig. 8. Effect of adsorption time on dye adsorption by gallic-MWCNTs **4**.

MWCNTs and gallic-MWCNTs **4**, respectively. Moreover, the q_e values of gallic-MWCNTs **4** were higher obviously than that of carboxyl MWCNTs for all tested dyes. These results suggested that the introduction of gallic units on MWCNTs enhanced the adsorption abilities markedly. In order to further study the kinetic mechanism of adsorption process, the pseudo-first-order and second-order models were used to analyze the experimental data of gallic-MWCNTs **4** as Eqs. (2) and (3) [24].

$$\text{Pseudofirst-order}: \frac{1}{q_t} = \frac{k_1}{q_e t} + \frac{1}{q_e} \tag{2}$$

$$\text{Pseudo second-order}: \frac{t}{q_t} = \frac{1}{k_2 q_e^2} + \frac{1}{q_e} t \tag{3}$$

where k_1 (min^{-1}) and k_2 (min^{-1}) are the adsorption rate constants, q_t and q_e are the amount adsorbed at time t (min) and at equilibrium, respectively, both in mmol/g.

The results of rate constants of first-order and second-order kinetics for four dyes were listed Table 1. The linear relationships with high correlation coefficients ($R \approx 1.000$) between t/q_t and t implied the adsorption processes were well in accordance with pseudo-second-order model. From the data of Figs. 7 and 8 and Table 1, it could be concluded that the introduction of gallic units onto MWCNTs was favorable for adsorption and the adsorption process followed the pseudo-second-order model. The possible reason was that the introduction of gallic units reduced the self-aggregating of MWCNT in water and formed more cavities, which enhanced the adsorption speed and abilities remarkably.

3.3. Adsorption isotherms

The adsorption isotherms of gallic-MWCNTs **4** for four dyes were studied and the results were shown in Fig. 9(a). The equilibrium adsorption capacities (q_e) increased rapidly with the increase in concentration of dyes at low C_e values. The q_e values kept stable when $C_e > 6$ mmol/L, indicating the saturation adsorption nearly. In order to discuss the adsorption behaviors further, Langmuir isotherm and Freundlich isotherm used extensively for analyzing the adsorption behaviors, were employed to fit the experimental data. The Langmuir isotherm equation has been successfully applied in many real monolayer adsorption processes with a finite number of identical sites. It is represented by Eq. (4) [25]:

$$\frac{C_e}{q_e} = \frac{C_e}{q_m} + \frac{1}{q_{mKL}} \tag{4}$$

where q_e and C_e are the amounts of adsorption (mmol/g) and the adsorbate concentration (mmol/L) at equilibrium, respectively. K_L is Langmuir constant and q_m is the maximum adsorption capacity.

Table 1
Kinetic parameters for dyes adsorption by gallic-MWCNTs **4**

Pseudo-first-order model			Pseudo-second-order model			
Dyes	k_1 (min^{-1}) (SD)	q_1 (mmol/g) (SD)	R^2	k_2 (g $mmol^{-1}$ min^{-1}) (SD)	q_2 (mmol/g) (SD)	R^2
OG	7.12 (0.73)	0.357 (0.02)	0.902	0.373 (0.14)	0.359 (0.01)	0.998
BP	9.64 (1.22)	0.316 (0.04)	0.861	0.289 (0.16)	0.320 (0.01)	0.998
NR	4.56 (0.45)	0.471 (0.01)	0.908	0.456 (0.17)	0.472 (0.01)	0.998
MB	5.09 (0.38)	0.446 (0.01)	0.945	0.438 (0.12)	0.446 (0.01)	0.998

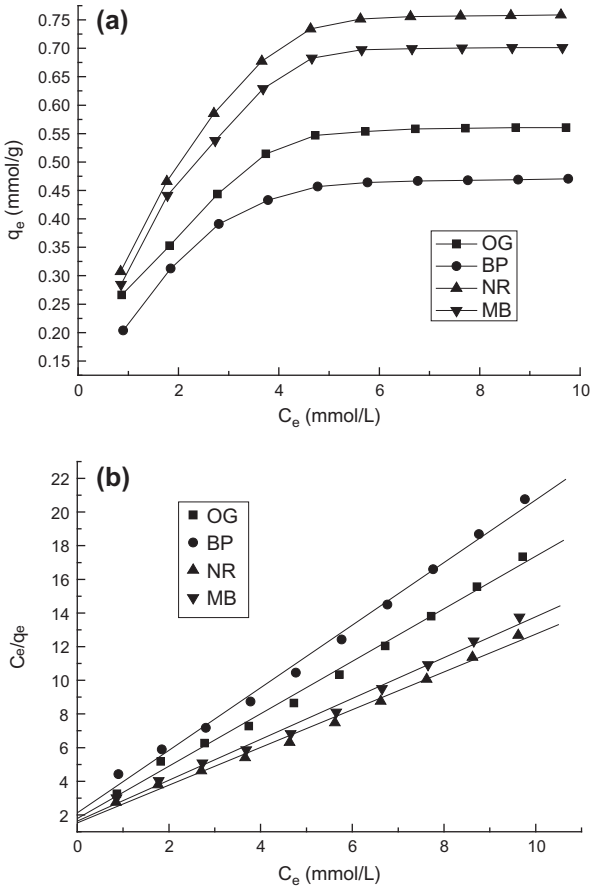

Fig. 9. Effect of initial concentration on dyes adsorption by gallic-MWCNTs **4**. (a) The plots of q_e against C_e and (b) the plots of C_e/q_e against C_e.

Freundlich isotherm equation for heterogeneous surfaces of multilayer adsorption is represented by Eq. (5) [26]:

$$\ln q_e = b_F \ln C_e + \ln K_F \quad (5)$$

Freundlich constants, K_F and b_F, can be calculated from a linear plot of ln q_e vs. ln C_e.

As shown in Fig. 9(b), the plots of C_e/q_e against C_e gave a straight line, suggesting that the adsorption processes of gallic-MWCNTs **4** for four dyes obeyed the Langmuir isotherm. Table 2 illustrated the adsorption isotherm constants for four dyes according to Eqs. (4) and (5). It can be seen the determination coefficient R^2 are relatively lower for Freundlich isotherms but near 1 for Langmuir isotherm. According to Langmuir isotherm, the adsorption capacities for four dyes (OG, BP, NR, MB) were 0.642 mmol/g (289 mg/g), 0.537 mmol/g (324 mg/g), 0.891 mmol/g (256 mg/g), and 0.823 mmol/g (310 mg/g), respectively. Comparing with the adsorption properties of unmodified MWCNT and other molecule-modified CNTs (as shown in Table 3), gallic-MWCNTs **4** presented outstanding adsorption capabilities for both cationic and anionic dyes [15,19,20,27–29]. Especially, the highest adsorption capabilities were as high as 324 mg/g for BP. The possible explanation for the excellent sorption was that the introduction of gallic units were favorable for preventing the self-aggregation of MWCNT in solvents and constructed more cavities for dyes sorption.

3.4. Adsorption thermodynamics

Adsorption thermodynamics can be used to estimate the inherent energy change of sorbent after adsorption. The adsorption behaviors at different temperatures (298, 308, and 318 K) were investigated by studying the dependence of Langmuir adsorption equilibrium constant with temperature. The standard Gibbs free energy change (ΔG), standard enthalpy change (ΔH), and standard entropy change (ΔS) were calculated by van't Hoff equation (6) and (7) [30]:

$$\ln K_L = -\frac{\Delta H}{RT} + \frac{\Delta S}{R} \quad (6)$$

$$\Delta G = \Delta H - T\Delta S \quad (7)$$

Table 2
Adsorption isotherm constants of gallic-MWCNTs **4** for dyes (K_L/L mmol^{-1}, q_m/mmol g^{-1}, K_F/mmol g^{-1}(L mol^{-1}), b_F)

	Langmuir adsorption isotherms constants			Freundlich adsorption isotherms constants		
Dyes	K_L (SD)	q_m (SD)	R^2	K_F (SD)	b_F (SD)	R^2
OG	0.873 (0.138)	0.642 (0.041)	0.997	0.303 (0.057)	0.316 (0.015)	0.953
BP	0.877 (0.137)	0.537 (0.049)	0.997	0.260 (0.066)	0.401 (0.026)	0.929
NR	0.737 (0.128)	0.891 (0.033)	0.996	0.374 (0.069)	0.367 (0.023)	0.949
MB	0.745 (0.134)	0.823 (0.036)	0.996	0.348 (0.070)	0.365 (0.043)	0.947

Table 3
Comparison of maximum adsorption capacity (q_{max}) of various CNTs sorbent for dyes

Dye	Sorbent	q_{max}(mmol/g, mg/g)	Reference
Orange G sodium salt	gallic-MWCNTs	0.642, 289	This work
Brilliant ponceau 5R	gallic-MWCNTs	0.537, 423	This work
Neutral red	gallic-MWCNTs	0.891, 256	This work
Methylene blue	gallic-MWCNTs	0.823, 310	This work
Methylene blue	cyclodextrin-CNTs	0.525, 196	[20]
Methyl orange	starch-CNTs	0.415, 136	[10]
Congo red	chitosan-CNTs	0.375, 261	[19]
Direct red 23	Fe_3C-CNTs	0.224, 172	[27]
Reactive Red M-2BE	bared MWCNTs	0.191, 188	[28]
Neutral red	guar gum-CNTs	0.313, 90	[29]
Methylene blue	bared MWCNTs	0.160, 59.7	[15]
AR183	bared MWCNTs	0.085, 45.2	[15]

Table 4
Thermodynamic parameters for dyes adsorption by gallic-MWCNTs **4**

	ΔH (kJ/mol)	ΔS (J/mol K)	ΔG (kJ/mol) 298 K	ΔG (kJ/mol) 308 K	ΔG (kJ/mol) 318 K
OG	−4.127	−11.22	−0.783	−0.671	−0.559
BP	−5.383	−12.32	−1.711	−1.588	−1.465
NR	−4.473	−9.35	−1.687	−1.587	−1.499
MB	−4.869	−9.981	−1.894	−1.794	−1.695

By plotting a graph of ln K_L vs. $1/T$, the values of ΔH, ΔS, and ΔG were calculated and listed in Table 4. It can be seen that all ΔH, ΔS, and ΔG were negative, which indicated that these adsorption behaviors were exothermic and spontaneous. These small values of ΔG on dye adsorption of MWCNTs were also reported in literature [31]. This phenomenon indicated that the adsorption were controlled by physisorption (−20 to 0 kJ/mol) and attained adsorption equilibrium nearly at the tested temperatures.

3.5. pH influences on adsorption capacities

In general, the pH values make great influences on adsorption. Thus, the adsorption capacities of gallic-MWCNTs **4** for four dyes were studied in the range of pH 3–10 (10 mL of dye solution, concentration at 2.0×10^{-3} M, 5.0 mg of sorbent, 24 h of adsorption time. The pH was adjusted by solution of HCl or solution of NaOH). The results were shown in Fig. 10. It can be seen that the adsorption capacities for anionic dyes (OG and BP) with sulfonic acid groups and hydroxyl groups decreased with the increase in the pH values of solution. However, the adsorption capacities for cationic dyes with ammonium groups (NR and MB) showed reverse change. These change trends were similar to the reports in literatures [13,31]. These results were also in accordance with the structures of dyes. The amine groups in cationic dyes of NR and MB are easily protonated at low pH values and the sulfonic groups and phenolic hydroxyl groups in anionic dyes of OG and BP are easily ionization at high pH values. The protonation and ionization enhanced the water solubility, resulting in the unfavorable influences on adsorption obviously.

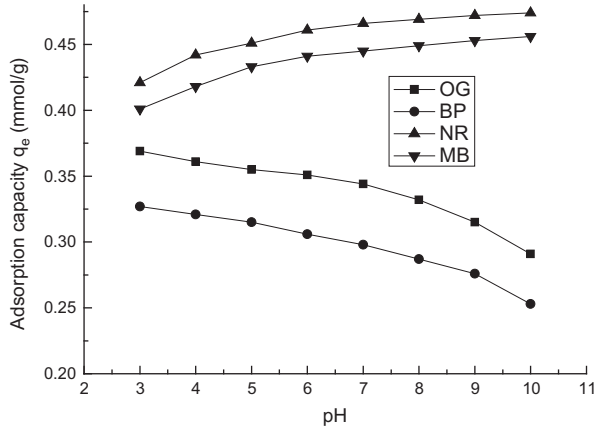

Fig. 10. The effect of pH on adsorption capacities.

3.6. The recycle adsorption property after desorption

The reused adsorption property of gallic-MWCNTs **4** was studied for MB as the representative one. After adsorption for MB (in the thermostatic shaker bath with a shaking of 200 rpm at 25°C for 6 h, 10 mL of dye solutions with concentration of 2.0×10^{-3} M, 5.0 mg of sorbent), the gallic-MWCNT **4** was desorbed by 10% HCl and subsequently 10% NaOH. Then it was washed adequately by distilled water and dried by vacuum. The obtained product was reused for dye adsorption again. The five times' adsorption percentages were measured and average of two independent experiments was carried out. The results were 0.337, 0.311, 0.291, 0.268, and 0.232 mmol/g, respectively. These high values of adsorption in five times' recycles suggested that gallic-MWCNTs **4** possessed good reused property.

4. Conclusions

In this paper, novel gallic-MWCNTs **4** was prepared by reacting acyl chloride-MWCNTs with gallic amino derivative containing three long alkyl chains. Its structure was confirmed by FTIR, Raman spectroscopy, XRD, SEM, and TG. The dyes adsorption experiments indicated the novel carbon nanomaterial showed excellent dyes adsorption capabilities than that of raw CNTs. The adsorption capacities of gallic-MWCNTs **4** for OG, BP, NR, and MB were 0.642 mmol/g (289 mg/g), 0.537 mmol/g (324 mg/g), 0.891 mmol/g (256 mg/g), and 0.823 mmol/g (310 mg/g), respectively. The adsorption kinetics was well in accordance with pseudo-second-order model. The adsorption processes were exothermic and spontaneous and obeyed the Langmuir isotherm equation.

Acknowledgments

Financial support from the National Natural Science Foundation of China (No.: 21406036), Fujian Natural Science Foundation of China (No. 2014J01034), Project of Fujian Provincial Department of Education (JA11044 and JA10056), and the Program for Innovative Research Team in Science and Technology in Fujian Province University were greatly acknowledged.

References

[1] A. Roy, B. Adhikari, S.B. Majumder, Equilibrium, kinetic, and thermodynamic studies of azo dye adsorption from aqueous solution by chemically modified lignocellulosic jute fiber, Ind. Eng. Chem. Res. 52 (2013) 6502–6512.

[2] I.T. Peternel, N. Koprivanac, A.M.L. Božić, H.M. Kušić, Comparative study of UV/TiO_2, UV/ZnO and photo-Fenton processes for the organic reactive dye degradation in aqueous solution, J. Hazard. Mater. 148 (2007) 477–484.

[3] G. Crini, P.M. Badot, Application of chitosan, a natural aminopolysaccharide, for dye removal from aqueous solutions by adsorption processes using batch studies: A review of recent literature, Prog. Polym. Sci. 33 (2008) 399–447.

[4] M.K. Purkait, S. DasGupta, S. De, Resistance in series model for micellar enhanced ultrafiltration of eosin dye, J. Colloid Interface Sci. 270 (2004) 496–506.

[5] S. Chakraborty, M.K. Purkait, S. DasGupta, S. De, J.K. Basu, Nanofiltration of textile plant effluent for color removal and reduction in COD, Sep. Purif. Technol. 31 (2003) 141–151.

[6] Y.R. Wang, W. Chu, Adsorption and removal of a xanthene dye from aqueous solution using two solid wastes as sorbent, Ind. Eng. Chem. Res. 50 (2001) 8734–8741.

[7] J. Hu, D.D. Shao, C.L. Chen, G.D. Sheng, X.M. Ren, X.K. Wang, Removal of 1-naphthylamine from aqueous solution by multiwall carbon nanotubes/iron oxides/cyclodextrin composite, J. Hazard. Mater. 185 (2011) 463–471.

[8] P. Xu, G.M. Zeng, D.L. Huang, C. Lai, M.H. Zhao, Z. Wei, N.J. Li, C. Huang, G.X. Xie, Adsorption of Pb(II) by iron oxide nanoparticles immobilized Phanerochaete chrysosporium: Equilibrium, kinetic, thermodynamic and mechanisms analysis, Chem. Eng. J. 203 (2012) 423–431.

[9] L. Eskandarian, M. Arami, E. Pajootan, Evaluation of adsorption characteristics of multiwalled carbon nanotubes modified by a poly(propylene imine) dendrimer in single and multiple dye solutions: Isotherms, kinetics, and thermodynamics, J. Chem. Eng. Data 59 (2014) 444–454.

[10] P.R. Chang, P.W. Zheng, B.X. Liu, D.P. Anderson, J.G. Yu, X.F. Ma, Characterization of magnetic soluble starch-functionalized carbon nanotubes and its application for the adsorption of the dyes, J. Hazard. Mater. 186 (2011) 2144–2150.

[11] J. Ghobadi, M. Arami, H. Bahrami, N. Mahmoodi, Modification of carbon nanotubes with cationic surfactant and its application for removal of direct dyes, Desalin. Water Treat. 52 (2014) 4356–4368.

[12] S.B. Wang, C.W. Ng, W.T. Wang, Q. Li, L.Q. Li, A comparative study on the adsorption of acid and reactive dyes on multiwall carbon nanotubes in single and binary dye systems, J. Chem. Eng. Data 57 (2012) 1563–1569.

[13] F.M. Machado, C.P. Bergmann, E.C. Lima, B. Royer, F.E. de Souza, I.M. Jauris, T. Calvete, S.B. Fagan, Adsorption of reactive Blue 4 dye from water solutions by carbon nanotubes: Experiment and theory, Phys. Chem. Chem. Phys. 14 (2012) 11139–11153.

[14] C.H. Wu, Adsorption of reactive dye onto carbon nanotubes: Equilibrium, kinetics and thermodynamics, J. Hazard. Mater. 144 (2007) 93–100.

[15] S. Wang, C.W. Ng, W. Wang, Q. Li, Z. Hao, Synergistic and competitive adsorption of organic dyes on multiwalled carbon nanotubes, Chem. Eng. J. 197 (2012) 34–40.

[16] Y. Yao, H. Bing, X. Feifei, C. Xiaofeng, Equilibrium and kinetic studies of methyl orange adsorption on multiwalled carbon nanotubes, Chem. Eng. J. 170 (2011) 82–89.
[17] Y. Yao, F. Xu, M. Chen, Z. Xu, Z. Zhu, Adsorption behavior of methylene blue on carbon nanotubes, Bioresour. Technol. 101 (2010) 3040–3046.
[18] J. Fan, Z. Shi, Y. Ge, Y. Wang, J. Wang, J. Yin, Mechanical reinforcement of chitosan using unzipped multiwalled carbon nanotube oxides, Polymer 53 (2012) 657–666.
[19] H.Y. Zhu, Y.Q. Fu, R. Jiang, J. Yao, L. Liu, Y.W. Chen, L. Xiao, G.M. Zeng, Preparation, characterization and adsorption properties of chitosan modified magnetic graphitized multi-walled carbon nanotubes for highly effective removal of a carcinogenic dye from aqueous solution, Appl. Surf. Sci. 285 (2013) 865–873.
[20] J. Cheng, P.R. Chang, P.W. Zheng, X.F. Ma, Characterization of magnetic carbon nanotube–cyclodextrin composite and its adsorption of dye, Ind. Eng. Chem. Res. 53 (2014) 1415–1421.
[21] M. Funahashi, A. Sonoda, Liquid-crystalline perylene tetracarboxylic acid bisimide bearing oligosiloxane chains with high electron mobility and solubility, Org. Electron. 13 (2012) 1633–1640.
[22] F.F. Yang, X.Y. Bai, B.T. Xu, H.Y. Guo, Triphenylene-modified chitosan: Novel high efficient sorbent for cationic and anionic dyes, Cellulose 20 (2013) 895–906.
[23] D.D. Shao, G.D. Sheng, C.L. Chen, X.K. Wang, M. Nagatsu, Removal of polychlorinated biphenyls from aqueous solutions using β-cyclodextrin grafted multiwalled carbon nanotubes, Chemosphere 79 (2010) 679–685.
[24] Z.H. Wang, B. Xiang, R.M. Cheng, Y.J. Li, Behaviors and mechanism of acid dyes sorption onto diethylenetriamine-modified native and enzymatic hydrolysis starch, J. Hazard. Mater. 183 (2010) 224–232.
[25] I. Langmuir, The adsorption of gases on plane surfaces of glass, mica and platinum, J. Am. Chem. Soc. 40 (1918) 1361–1403.
[26] C.H. Giles, D. Smith, A. Huitson, A general treatment and classification of the solute adsorption isotherm. I. Theoretical, J. Colloid Interface Sci. 47 (1974) 755–765.
[27] W. Konicki, I. Pełech, E. Mijowska, I. Jasińska, Adsorption of anionic dye Direct Red 23 onto magnetic multi-walled carbon nanotubes-Fe_3C nanocomposite: Kinetics, equilibrium and thermodynamics, Chem. Eng. J. 210 (2012) 87–95.
[28] F.M. Machado, C.P. Bergmann, T.H.M. Fernandes, E.C. Lima, B. Royer, T. Calvete, S.B. Fagan, Adsorption of Reactive Red M-2BE dye from water solutions by multi-walled carbon nanotubes and activated carbon, J. Hazard. Mater. 192 (2011) 1122–1131.
[29] L. Yan, P.R. Chang, P.W. Zheng, X.F. Ma, Characterization of magnetic guar gum-grafted carbon nanotubes and the adsorption of the dyes, Carbohydr. Polym. 87 (2012) 1919–1924.
[30] C.Y. Chen, J.C. Chang, A.H. Chen, Competitive biosorption of azo dyes from aqueous solution on the templated crosslinked-chitosan nanoparticles, J. Hazard. Mater. 185 (2011) 430–441.
[31] W. Konicki, I. Pełech, E. Mijowska, I. Jasińska, Adsorption kinetics of acid dye Acid Red 88 onto magnetic multi-walled carbon nanotubes-Fe 3 C NANOCOMPOSITE, CLEAN—Soil, Air, Water 42 (2014) 284–294.